



# HHS Public Access

Author manuscript

*Biol Psychiatry Cogn Neurosci Neuroimaging*. Author manuscript; available in PMC 2020 May 01.

Published in final edited form as:

*Biol Psychiatry Cogn Neurosci Neuroimaging*. 2019 May ; 4(5): 434–443. doi:10.1016/j.bpsc.2018.01.003.

## Cortical morphometry in the psychosis risk period: A comprehensive perspective of surface features

Kate Damme<sup>1</sup>, Tina Gupta<sup>1</sup>, Robin Nusslock<sup>1</sup>, Jessica A. Bernard<sup>2,3</sup>, Joseph M. Orr<sup>2,3</sup>, and Vijay Mittal<sup>1</sup>

<sup>1</sup>Department of Psychology, Northwestern University

<sup>2</sup>Department of Psychological and Brain Sciences, Texas A&M University

<sup>3</sup>Texas A&M Institute for Neuroscience, Texas A&M University

### Abstract

**Background**—Gyrification features reflect brain development in the early prenatal environment. Clarifying the nature of these features in psychosis can help shed light on the role of early developmental insult. However, the literature is currently widely discrepant, which may reflect confounds related to formally psychotic patient populations or overreliance on a single cortical surface morphometry(CSM) feature.

**Methods**—The present study compares CSM features of gyrification in clinical high-risk (CHR, n=43) youth during the prodromal risk period to typically developing controls over two time points across three metrics; local gyrification index(LGI), mean curvature index(MCI), and sulcal depth (improving resolution and examination of change over 1-year).

**Results**—Gyrification was stable over time, supporting that gyrification reflects early insult rather than abnormal development/reorganization associated with the disease state. Each of the indices highlighted unique, aberrant features in the CHR group with respect to controls. Specifically, LGI reflected hypogyrfication in lateral orbitofrontal, superior bank of the superior temporal sulcus, anterior isthmus of the cingulate, and temporal poles; MCI indicated sharper gyral and flatter/wider sulcal peaks in the cingulate, post-central, and lingual gyrus; sulcal depth identified shallow features in parietal, superior temporal sulcus, and cingulate regions. Further, both MCI and sulcal depth converged on abnormal features in the parietal cortex.

**Conclusions**—Gyrification metrics suggest early developmental insult and provides support for neurodevelopmental hypotheses. Observations of stable CSM features across time provide context for interpreting extant studies and speak to CSM as a promising stable marker/endophenotype. Collectively, findings support the importance of considering multiple CSM features.

---

**Corresponding Author:** Katherine Damme, Department of Psychology, Northwestern University, 2029 Sheridan Rd., Evanston, IL 60208, Tel: 402-890-3606, Kate.Damme@u.northwestern.edu.

**Publisher's Disclaimer:** This is a PDF file of an unedited manuscript that has been accepted for publication. As a service to our customers we are providing this early version of the manuscript. The manuscript will undergo copyediting, typesetting, and review of the resulting proof before it is published in its final citable form. Please note that during the production process errors may be discovered which could affect the content, and all legal disclaimers that apply to the journal pertain.

### Financial Disclosure

All authors report no biomedical financial interests or potential conflicts of interest.

## Keywords

Cortical Surface; Morphometry; Schizophrenia; Prodrome; Psychosis; Gyrfication; Sulcal Depth; Curvature Index

---

## BACKGROUND

Cortical surface morphometry (CSM) may provide critical insight into the timing of developmental insults or pathogenic factors that contribute to psychotic disorders (1,2). Indeed gyrification, a CSM feature parametrized by local gyrification index (*GI*), mean curvature index (*MCI*), and sulcal depth may reflect abnormal connectivity in utero and in early development, as cortical folding reflects late 2<sup>nd</sup> and 3<sup>rd</sup> trimester integrity of cortico-cortical and subcortical connectivity (1,2). Gyrfication measured in late adolescence and early adulthood may be relatively unchanged by adolescent neuromaturational processes that drive instability in other cortical features (3). This relative stability suggests that gyrfication metrics may provide unique insight into the contribution of early development to risk for psychosis (2,3).

Unfortunately, little is known about the contributions of early brain development to psychosis because clinical markers of psychosis often appear in late adolescence to early adulthood when neuromaturational processes have already obscured early development (3). Indirect evidence suggests a link between early brain development and increased rates of psychosis from prenatal famine/nutrition (4,5), flu exposure (6, 7), and deletions of genes related to early brain development (i.e., 22q11 deletion; 8,9). Furthermore, other established markers of early prenatal development (e.g., dermatoglyphics) relate to psychosis (10,11), but do not provide a direct metric of brain development. Gyrfication may provide a more direct metric of early brain development and added insight into abnormal neurodevelopmental processes in psychosis.

With regard to schizophrenia, the CSM literature is inconsistent (12–14). These inconsistencies may be due in part to variations in methodological approaches and confounds associated with schizophrenia (e.g. substance dependence and medications) (15–17). As a result, it is unknown if gyrfication abnormalities reflect early insult alone and remain unchanged during the prodromal period. Alternatively, gyrfication may be subject to later neurodegenerative or putative factors such as medication or substance abuse. If stable, gyrfication would provide an early marker of prenatal insult that is stable across pubertal neuromaturation. Additionally, gyrfication metrics may confer additional sensitivity to detecting risk for psychosis, thus adding insight from prenatal development that compliments structural metrics of prodromal neural reorganization (e.g. cortical thickness) (18–20).

Evaluating clinical high risk (CHR) populations (i.e., youth exhibiting prodromal syndromes indicating imminent risk for psychotic disorders prior to psychosis onset) can provide predictive biomarkers as well as insight into pathogenic processes. While this group does exhibit some of the same types of confounds as seen in patients with schizophrenia overall; individuals in this period tend to show fewer factors that convolute results compared to

chronic psychosis populations (e.g., medication rates and doses are often lower). With respect to CSM, the few studies that focus on CHR populations do indicate surface abnormalities in these individuals (15–16,21–22). Nevertheless, there is no comprehensive understanding of CSM in CHR individuals, as these investigations rely on a single CSM metric at a single time point (see Supplemental Information (SI) for a review and comparison of metrics). Examining multiple time points of CSM features may establish whether gyrification reflects a pre-existing early insult or pathogenic processes during the CHR period. This approach may provide insight into these features in schizophrenia and spectrum populations; specifically, this will help to determine if CSM features are sensitive to neurodegenerative processes or putative environmental factors (See Table 1; See SI for review of relevant literature).

The current study evaluates three metrics of gyrification: local gyrification index, mean curvature index, and sulcal depth. Local gyrification index ( $\mathcal{LGI}$ ), is the ratio of an outer surface contour to buried cortical surface which employs advanced computation in three-dimensions of gyrification rather than relying on a single orientation such as gyrification index (GI) (23–24). While the  $\mathcal{LGI}$  provides invaluable information, it references an individualized contour; taking this approach in isolation may obscure the exact nature of the specific gyral morphometry. A solution to this issue may lie in incorporating additional measures such as mean curvature index (MCI). MCI quantifies each vertex in terms of the radius of osculating circles from the peak of each gyrus (25). This CSM metric provides further sensitivity to changes on a smaller scale and information about the shape of a given arch (i.e. higher MCI implies a sharper curve while lower numbers represent a wider arch; 26). Finally, sulcal depth provides unique and complimentary estimates of linear distance from a reference midpoint surface (i.e. the global midpoint between the gyri and sulci; 27). Thus, incorporating three metrics provides a more comprehensive and nuanced perspective, which includes an inner/outer surface ratio, a curve reference, and linear height/depth.

By incorporating data across two scan sessions and combining complementary indices ( $\mathcal{LGI}$ , MCI, and sulcal depth) in a single population, we provide a more comprehensive account of CSM differences (See SI for a review of metrics) in CHR individuals. In addition, the present study benefits from incorporating data from two scan sessions, an approach that improves the likelihood of accounting for additional variance and noise (e.g., the variance in gyrification related to scan slice angle in image acquisition) (17, 24) and stability of CSM variables. Further, examining CSM features over time allows for a novel perspective that clarifies if CSM features reflect a stable vulnerability trait or something that shifts as a function of pathogenic processes in the CHR period.

In the present investigation, 81 participants (43 CHR and 38 healthy control; HC) completed clinical interviews, a structural scan at a baseline, and then a second follow-up scan 12 months later. We evaluated gyrification features from large scale folding ratios ( $\mathcal{LGI}$ ), shape of the curve (mean curvature index; MCI), and the height/depth of gyri and sulci (sulcal depth) in both groups (see SI). We predicted that these CSM features develop in utero and are relatively insensitive to developmental and environmental factors. Past findings suggested both hyper- and hypo-gyrification in schizophrenia (12,14,28). Similarly, gyrification index, folding index, and  $\mathcal{LGI}$  studies in CHR youth indicate widespread aberrant

gyrification (15–16, 21, 29–32), with little convergence outside of frontal and temporal regions. From this literature, we predicted that CHR youth will show aberrant  $\mathcal{GI}$  in frontal and temporal regions. There is no current guiding literature on curvature, and so we investigated curvature with exploratory analyses. Based on limited evidence in the olfactory cortex indicating shallow sulcal depth in CHR youth (22), we predicted shallower peaks and depths for sulcal depth. Further, we predicted that there would be no difference in slope between time-points, indicating the relative stability of gyrification over time. Finally, we aimed to examine how the features relate to one another; any areas of overlap (where CHR shows abnormalities compared to HC) were evaluated in both a quantitative and qualitative fashion.

## METHODS

A total of 81 participants (CHR=43, HC=38) were recruited through the Adolescent Development and Preventive Treatment (ADAPT) Program. CHR inclusion criteria was based on the presence of a prodromal syndrome (33) and not genetic risk. Demographic and positive symptoms characteristics of the sample are described in Table 2 (See SI for exclusion and recruitment criteria). The Structured Interview for Prodromal Syndromes (SIPS; 34) was used to diagnose CHR syndromes. Participants were also given the Word Reading subtest of the fourth edition of the Wide Range Achievement Test (WRAT) as a measure of general intelligence. The WRAT is well-validated and broadly used measure of achievement and broad learning ability for adolescents and young adults (35).

A 3-Tesla Siemens Tim Trio MRI Scanner (Siemens AG, Munich, Germany) using a standard 12-channel head coil acquired two scans approximately one year apart. Structural images were collected on a T1-weighted 3D magnetization prepared rapid gradient multi-echo sequence (MPRAGE; sagittal plane; repetition time [TR] 2,530 ms; echo times [TE] 51.64 ms, 3.5 ms, 5.36 ms, 7.22 ms, 9.08 ms; GRAPPA parallel imaging factor of 2; 1 mm<sup>3</sup> isotropic voxels, 192 interleaved slices; FOV 525 6 mm; flip angle 57). Query Design Estimate Contrast tool (QDEC) in the FreeSurfer 6.0 program generated the group contrasts in a general linear model controlling for gender and medication status, and compared MCI and sulcal depth at each vertex. Local gyrification index was calculated using the general linear model tools (24, For full data acquisition parameters and preprocessing see Supplemental Information). QDEC in the FreeSurfer program generated the group contrasts in a repeated measure ANOVA, controlling for gender and medication status, compared MCI and sulcal depth at each vertex. To examine gyrification stability, an Inter-Class Correlation (ICC) compared the CSM metrics for each time point for significant clusters to reduce the number of comparisons to the relevant vertices discussed below. These analyses treat FreeSurfer's standardized algorithm as a single, stable rater of CSM metrics in a fixed-rater model of class correlation, which was used in the Psych Package of R v.3.1.2 (36). While Cronbach's Alpha is typically reported, Guttman's Lambda has been reported here as it better takes into account the variance of the data (36; See SI for full description).

## RESULTS

### Group Comparison of the Cortical Surface Morphometry Gyrfication Metrics

In a whole brain analyses, the CHR and HC groups differed in gyrfication (FDR-corrected  $p < .05$ , across both hemispheres and Bonferroni corrected for three metric comparisons). The analyses revealed six significant clusters where the  $\mathcal{I}GI$  differed by group controlling for gender and antipsychotic status (Figure 1, Table 3). In the left hemisphere, the CHR group showed a decreased  $\mathcal{I}GI$ , or reduction in the outer surface to inner surface signifying less gyrfication, in the bank of the superior temporal sulcus and the temporal pole. In the right hemisphere, the CHR group showed a reduction in  $\mathcal{I}GI$ -less gyrfication- in the lateral orbitofrontal, bank of the superior temporal sulcus, parahippocampal gyrus, and fusiform. Interestingly, no clusters demonstrated increased gyrfication in the CHR group suggesting hypogyrfication in the CHR group compared to the HC group.

Whole brain analyses revealed nine significant clusters where MCI differed by group (Figure 2, Table 4). For many regions on the left hemisphere, the CHR group demonstrated a decreased MCI, or sharper gyral curves, in the lingual gyrus, inferior parietal lobule, and postcentral gyrus. A single left hemisphere cluster demonstrated opposing results with the fusiform gyrus showing sharper gyrfication in the CHR group. In the right hemisphere, the CHR group showed a decrease MCI with decreased peak angles in the superior parietal lobule, isthmus cingulate, and superior parietal lobule. A single right hemisphere cluster demonstrated opposing results in a sulcus of the superior parietal lobule showing sharper gyrfication in the CHR group.

In each hemisphere, the CHR and HC groups differed in sulcal depth. The analyses revealed nine significant clusters where sulcal depth differed by group controlling for gender and antipsychotic status (Figure 3, Table 5). In the left hemisphere, the CHR showed decreased sulcal depth, or gyral height from the cortical midpoint, in the postcentral gyrus, posterior cingulate, rostral middle frontal gyrus, and lingual gyrus. Again, there was a single cluster of increased sulcal depth on the fusiform gyrus. In the right hemisphere, the CHR had decreased sulcal depth in gyral areas of the superior parietal lobule and anterior cingulate with a single cluster of increased sulcal depth in the UHR group in the superior parietal lobule.

### Comparison of Cortical Surface Morphometry Across Metrics and Time

To evaluate whether CSM clusters converge on vertices or identify unique vertices of surface morphometry, significant clusters were overlaid pairwise, generating two unique masks: a convergence map (containing vertices where metrics overlap on CSM abnormalities) and a uniqueness map (demonstrating the unique information provided by each metric) (Table 5, Figure 4). Spatial convergence of significant voxels only occurred between two metrics, MCI (19.5% of vertices overlap in the left hemisphere; 28.72% of vertices overlap in the right hemisphere) and abnormal sulcal depth (34.61% of vertices overlap in the left hemisphere; 26.44% of vertices overlap in the right hemisphere). Qualitatively, while the ratio metric of  $\mathcal{I}GI$  demonstrated distinct gyrfication in frontal and temporal regions, the

geometric distance and shape metrics, MCI and sulcal depth, clusters were primarily in parietal, occipital, and cingulate regions, Supplemental Table 1.

In order to use both time points as a converging data point, we tested the assumption that the gyrification is stable over time. These time points also provided us with a unique opportunity to confirm the stability of gyrification and assess whether these metrics changed during the prodromal period. Across all subjects the CSM metrics were significantly and highly stable over time (See SI). These measures were also highly reliable:  $\mathcal{K}GI$  ( $\Lambda=.92$ ), MCI ( $\Lambda=.86$ ), and sulcal depth ( $\Lambda=.93$ ). In parallel analyses, the CHR group did not significantly vary in the stability of their CSM, Supplemental Table 2. Follow-up analyses compared peak clusters to symptoms, see SI and Supplemental Table 3.

## CONCLUSIONS

The present study was highly innovative in examining a number of CSM characteristics over two time points (one year apart) during the CHR period. This approach yielded several important findings. First, CSM characteristics appeared highly stable over time, which has relevance for informing conceptual models of psychosis. Next, we observed distinct abnormalities in CSM features across cingulate, parietal, orbital frontal, and superior temporal regions. Further, we detected converging clusters of aberrant CSM matrixes, converging on the parietal lobule. Taken together, this novel approach was effective in providing a comprehensive perspective that yielded new discoveries about CSM features. Specifically, each index highlighted unique aberrant features in the CHR group, which would have been missed if we had employed a single variable approach. With  $\mathcal{K}GI$ , CHR participants exhibited hypogyrfication in lateral orbitofrontal cortex, superior bank of the superior temporal sulcus, anterior isthmus of the cingulate, and temporal poles. In terms of curvature, the CHR youth had both sharper peaks on the gyri and flatter/wider sulcal peaks in the posterior isthmus of the cingulate, post-central gyrus, and the lingual gyrus. In terms of sulcal depth, we observed shallower overall gyrification in the CHR youth with distinct local parietal, parietal opericulum, inferior bank of the superior temporal sulcus, and rostral cingulate regions.

In line with predictions, there was abnormal gyrification in the CHR group in the temporal and frontal lobes. The evaluation of  $\mathcal{K}GI$  identified entirely spatially unique clusters where groups differed. The distinct spatial and conceptual information (i.e., local ratios rather than linear or arc metric) provided by this metric highlights the importance integrating multiple metrics of CSM features. The CHR group demonstrated hypo-gyrification compared to the HC group and this finding is consistent with reports from other studies of CHR participants. Bakker et al. (2016) found a similar hypogyrfication pattern that was predictive of later symptoms (37). Similarly, Hirjak et al. (2015), found clinical features related to aberrant gyrification along the bank of the superior temporal sulcus, a region that was also identified in the current study (38). Finally, these findings are consistent with single time point analyses of CHR (31–32), first episode psychosis (31–32), and schizophrenia (39), who found similar patterns of gyrification temporal, frontal, and parahippocampal regions when compared to controls.



Group comparisons of MCI, an understudied metric of gyrification, revealed distinct parietal geometry of gyrification related to the CHR group. This metric indicated many clusters in the parietal lobe, demonstrating steeper, sharper curves on the edge of gyri and wider curves within the sulci. While no previous studies of CHR individuals have investigated MCI, studies of schizophrenia do demonstrate a pattern of parietal sulcal curvature distinct from controls (40). Drawing instead from related work in connectivity (41), and other metrics of gyrification (31–32,39), there was ample evidence relating superior temporal, orbitofrontal, cingulate, and parietal regions in psychosis in adolescence, but none of this has been taken directly from MCI. Here, we provided further support for the notion that MCI may be a useful metric of pathological early development, identifying distinct CHR cingulate curvature features not yet identified in the literature. Importantly, MCI was sensitive to the CSM features that would not have been identified by examining  $\mathcal{M}GI$  alone. While several MCI features converged with sulcal depth to identify surface features that distinguished between CHR and HC groups, 76.4% of voxels identified by MCI were unique. This MCI specific pattern highlighted again the importance of a comprehensive approach to analyzing CSM features. Furthermore, while common CSM feature sites were identified, each metric provided unique conceptual information about these voxel sites. Specifically, MCI identified distinct shape features of curvature, but provided no insight into the gray matter to white matter ratio or height or depth of gyri and sulci.

The sulcal depth group analysis indicated aberrant structure in the CHR group, largely in parietal, opercular, and cingulate regions. While the only CHR study of sulcal depth focused on a region of interest in the olfactory sulcus (22), the current parietal pattern of sulcal depth abnormalities is consistent with findings that identified postcentral and parietal opercular regions of aberrant sulcal depth in schizophrenia (42). While many CSM features overlapped with the features identified by MCI, several of the sulcal depth metrics clusters were distinct in their identification of critical clusters. Additionally, sulcal depth provided unique information about these clusters. MCI indicated that parietal clusters fall away more steeply into wider sulcal curves, and sulcal depth findings suggested that these curves were also shallower in sulcal depth. Taken together, the HC group had both higher gyri and lower sulci compared to CHR in these clusters.

The neural diathesis-stress conceptualization of psychosis suggests genetic factors and early developmental insults confer early vulnerability for psychosis. Then later, in adolescence, this pre-existing aberrant CSM feature vulnerability interacts with neuromaturational factors. This interaction of early and neuromaturational factors – both normative and pathological brain development – eventually form psychotic symptoms (20,43–44). Examining the adolescent period immediately preceding onset yielded many important findings. However, our understanding of both the early insult period, and how early insult later interacts with pubertal factors, is limited.

The present findings provide two important advancements in this regard. First, youth meeting criteria for a prodromal syndrome did, in fact, show marked brain characteristics that may speak to an early insult, as CSM features developed and harden in response to connectivity. Second, the present results provided a new perspective on the stability of CSM features across adolescent neuromaturational processes in both CHR individuals and

controls. While gyrification developed in tandem with brain connectivity in utero (45), the majority of studies emphasized neural development in the adolescent prodromal period (29; 46). The vast adolescent neuromaturational changes led researchers to question if CSM features undergo further changes in the prodrome or after onset (15–16). Additionally, present findings suggest that gyrification was remarkably static, which has implications for the way we view stable versus changing vulnerability factors in a period of active normative and pathological development. Additionally, these findings may impact the way we interpret findings in the context of leading neurodevelopmental (20,44) and disconnectivity conceptualizations of psychosis (18). Finally,  $\mathcal{GI}$  is a potential early biomarker of risk, distinguishing CHR, psychosis converters, and FEP from healthy controls (15–16,30–32). In this regard, CSM gyrification metrics may have added value when combined with gray matter and white matter changes over adolescence in identifying risk and predicting conversion with techniques like machine learning classification. Additionally, connectomics across metrics of gyrification may refine prediction and individualization of treatment (39).

Altogether, it is particularly interesting that areas that develop earlier (i.e., visual and parietal regions) showed aberrant curvature and sulcal depth, while  $\mathcal{GI}$  clusters tended towards later developing regions (i.e., frontal lobe and temporal areas). This distinction may be driven by the content of the metrics, as both sulcal depth and MCI exclusively measure gray matter surface features, while  $\mathcal{GI}$  measures is also sensitive to the white matter surface. Therefore, it is possible that our findings in the parietal lobule are reflective of abnormal brain development and connectivity in utero, while the broader regions implicated by  $\mathcal{GI}$  may be also picking up on aberrant white matter surface features that occurred later in development (myelination). However, it will be important for future larger longitudinal studies with more developmental times points, to confirm this possibility. Further, it will be important for future studies to consider how these features contribute uniquely to behavioral and cognitive aspects of psychosis. Additionally, future research should examine measures of prenatal environment as it relates to CSM features such as substance use, measures of stress, parental education, parental socioeconomic status, urbanicity (47), obstetric complications, or neurological soft signs such as motor impairment may relate to CSM features (48). It is also important to examine the relationship between gyrification and potentially related metrics such as connectivity and cortical gray matter and white matter volumetrics. Collectively, the findings, indicating substantives novel contributions from each index, support a recommendation that all future studies of CSM features include multiple indices. Furthermore, it will be necessary to investigate conversion longitudinally in separate investigations as this could be an informative empirical question to psychosis and cortical morphology broadly.

This study shows great promise but there are also still important limitations to consider. While the present study sample is comparable to, or larger than, other longitudinal studies (17–37 people;15–16,30,49–52), future work could benefit from increased sample sizes. Notably, this represents one of the largest studies in a CHR population to include two scan time points (15–16,30). Additionally, moving forward it will be important to understand the relationship between CSM features and antipsychotic medication use. While some CSM features, i.e. gray matter volume, are sensitive to antipsychotic medication (53–58), it remains unclear if gyrification is stable across treatment. The present study only included a



small number of the CHR participants treated with antipsychotic medications (n=8) and did not find a significant effect of medication. Nonetheless, the influence of neuroleptic treatment on cortical and subcortical structure remains an important empirical question and future work, with better powered studies, should continue to evaluate medication effects of CSM features. Further, the present study included an uneven gender distribution between groups (in part reflecting the nature of psychosis), and while we did not detect any effects for sex, future work should carefully evaluate possible sex differences.

## Supplementary Material

Refer to Web version on PubMed Central for supplementary material.

## Acknowledgments

This work was supported by the National Institute of Mental Health [2T32MH067564] to K.S.D. and the project was supported by National Institute of Health RO1MH094650, 1R01MH112545-01 R21/R33MH103231 and R21MH110374 to V.A.M.

## References

1. Van Essen DC. 1997; A tension-based theory of morphogenesis and compact wiring in the central nervous system. *Nature*. 385(6614):313–318. DOI: 10.1038/385313a0 [PubMed: 9002514]
2. White T, Hilgetag CC. 2011; Gyrfication and neural connectivity in schizophrenia. *Development and Psychopathology*. 23(1):339–352. DOI: 10.1017/S0954579410000842 [PubMed: 21262059]
3. Li G, Wang L, Shi F, Lyall AE, Lin W, Gilmore JH, Shen D. 2014; Mapping longitudinal development of local cortical gyrfication in infants from birth to 2 years of age. *The Journal of Neuroscience*. 34(12):4228–4238. [PubMed: 24647943]
4. Brown AS, Susser ES. 2008; Prenatal nutritional deficiency and risk of adult schizophrenia. *Schizophrenia Bulletin*. 34(6):1054–1063. [PubMed: 18682377]
5. Mackay E, Dalman C, Karlsson H, Gardner RM. 2017; Association of gestational weight gain and maternal body mass index in early pregnancy with risk for nonaffective psychosis in offspring. *JAMA Psychiatry*. 70(4):339–349.
6. Mednick SA, Machon RA, Huttunen MO, Bonett D. 1988; Adult schizophrenia following prenatal exposure to an influenza epidemic. *Arch Gen Psychiatry*. 45(2):189–192. [PubMed: 3337616]
7. Brown A. 2006; Prenatal infection as a risk factor for schizophrenia. *Schizophrenia Bulletin*. 32(2): 200–202. [PubMed: 16469941]
8. Simon TJ, Ding J, Bish JP, McDonald-McGinn DM, Zackai EH, Gee J. 2005; Volumetric, connective, and morphologic changes in the brains of children with chromosome 22q11.2 deletion syndrome: An integrative study. *Neuroimage*. 25(1):169–180. [PubMed: 15734353]
9. Gur RE, Bassett AS, McDonald-McGinn DM, Bearden CE, Chow E, Emanuel BS, Owen M, et al. 2017; A neurogenetic model for the study of schizophrenia spectrum disorders: The international 22q11.2 deletion syndrome brain behavior consortium. *Molecular Psychiatry*. 22(12)doi: 10.1038/mp.2017.161
10. Mittal VA, Dean DJ, Pelletier A. 2012; Dermatoglyphic asymmetries and fronto-striatal dysfunction in young-adults reporting non-clinical psychosis. *Acta Psychiatrica Scandinavica*. 126(4):290–297. DOI: 10.1111/j.1600-0447.2012.01869.x [PubMed: 22519833]
11. Russak ODF, Ives L, Mittal VA, Dean DJ. 2016; Fluctuating dermatoglyphic asymmetries in youth at ultrahigh-risk for psychotic disorders. *Schizophrenia Research*. 170(0):301–303. DOI: 10.1016/j.schres.2015.12.013 [PubMed: 26723845]
12. Kulynych JJ, Luevano LF, Jones DW, Weinberger DR. 1997; Cortical abnormality in schizophrenia: An in vitro application of the gyrfication index. *Biological Psychiatry*. 41(10):995–999. DOI: 10.1016/S0006-3223(96)00292-2 [PubMed: 9129779]

13. Palaniyappan L, Liddle PF. 2012; Differential effects of surface area, gyrification and cortical thickness on voxel based morphometric deficits in schizophrenia. *NeuroImage*. 60(1):693–699. DOI: 10.1016/j.neuroimage.2011.12.058 [PubMed: 22227049]
14. Palaniyappan L, Mallikarjun P, Joseph V, White TP, Liddle PF. 2011; Folding of the prefrontal cortex in schizophrenia: Regional differences in gyrification. *Biological Psychiatry*. 69(10):974–979. DOI: 10.1016/j.biopsych.2010.12.012 [PubMed: 21257157]
15. Harris JM, Whalley H, Yates S, Miller P, Johnstone EC, Lawrie SM. 2004; Abnormal cortical folding in high-risk individuals: A predictor of the development of schizophrenia? *Biological Psychiatry*. 56(3):182–189. DOI: 10.1016/j.biopsych.2004.04.007 [PubMed: 15271587]
16. Harris JM, Yates S, Miller P, Best JJK, Johnstone EC, Lawrie SM. 2004; Gyrification in first-episode schizophrenia: A morphometric study. *Biological Psychiatry*. 55(2):141–147. DOI: 10.1016/S0006-3223(03)00789-3 [PubMed: 14732593]
17. Narr KL, Toga AW, Szeszko P, Thompson PM, Woods RP, Robinson D, et al. 2005; Cortical thinning in cingulate and occipital cortices in first episode schizophrenia. *Biological Psychiatry*. 58(1):32–40. DOI: 10.1016/j.biopsych.2005.03.043 [PubMed: 15992520]
18. Friston K, Brown HR, Siemerkus J, Stephan KE. 2016; The dysconnection hypothesis (2016). *Schizophrenia Research*. 176(2–3):83–94. DOI: 10.1016/j.schres.2016.07.014 [PubMed: 27450778]
19. Friston KJ, Frith CD. 1995; Schizophrenia: A disconnection syndrome? *Clinical Neuroscience (New York, N.Y.)*. 3(2):89–97.
20. Walker E, Mittal V, Tessner K. 2008; Stress and the hypothalamic pituitary adrenal axis in the developmental course of schizophrenia. *Annual Review of Clinical Psychology*. 4(1):189–216. DOI: 10.1146/annurev.clinpsy.4.022007.141248
21. Jung WH, Kim JS, Jang JH, Choi JS, Jung MH, Park JY, Kwon JS. 2011; Cortical thickness reduction in individuals at ultra-high-risk for psychosis. *Schizophrenia Bulletin*. 37(4):839–849. DOI: 10.1093/schbul/sbp151 [PubMed: 20026559]
22. Takahashi T, Nakamura Y, Nakamura K, Ikeda E, Furuichi A, Kido M, et al. 2013; Altered depth of the olfactory sulcus in first-episode schizophrenia. *Prog Neuropsychopharmacol Biol Psychiatry*. 40:167–172. [PubMed: 23063493]
23. Zilles K, Armstrong E, Schleicher A, Kretschmann H. 1988; The human pattern of gyrification in the cerebral cortex. *Anatomy and Embryology*. 179(2):173–179. [PubMed: 3232854]
24. Schaer M, Cuadra MB, Schmansky N, Fischl B, Thiran JP, Eliez S. How to measure cortical folding from MR images: A step-by-step tutorial to compute local gyrification index; *Journal of Visualized Experiments*. 2012. 1–10.
25. Pienaar R, Fischl B, Caviness V, Makris N, Grant PE. 2008; A methodology for analyzing curvature in the developing brain from preterm to adult. *International journal of Imaging Systems and Technology*. 18(1):42–68. [PubMed: 19936261]
26. Luders E, Thompson PM, Narr KL, Toga AW, Jancke L, Gaser C. 2006; A curvature-based approach to estimate local gyrification on the cortical surface. *Neuroimage*. 29(4):1224–1230. [PubMed: 16223589]
27. Fischl B. 2012; *Freesurfer*. *Neuroimage*. 62(2):774–781. [PubMed: 22248573]
28. Wiegand LC, Warfield SK, Levitt JJ, Hirayasu Y, Salisbury DF, Heckers S, et al. 2005; An in vivo MRI study of prefrontal cortical complexity in first-episode psychosis. *Am J Psychiatry*. 162(1):65–70. [PubMed: 15625203]
29. Cannon TD, Chung Y, He G, Sun D, Jacobson A, Van Erp TGM. 2015 Progressive reduction in cortical thickness as psychosis develops: A multisite longitudinal neuroimaging study of youth at elevated clinical risk. *Biological Psychiatry*.
30. Harris JM, Moorhead TWJ, Miller P, McIntosh AM, Bonnici HM, Owens DGC, Lawrie SM. 2007; Increased prefrontal gyrification in a large high-risk cohort characterizes those who develop schizophrenia and reflects abnormal prefrontal development. *Biological Psychiatry*. 62(7):722–729. DOI: 10.1016/j.biopsych.2006.11.027 [PubMed: 17509536]
31. Sasabayasi D, Takayanagi T, Koike S, Yamasue H, Naoyuki K, Sakuma A, et al. 2017; Increased occipital gyrification and development of psychosis disorders in individuals with an at-risk mental state: A multicenter study. *Biological Psychiatry*. 8210:737–745. [PubMed: 28709499]

32. Sasabayasi D, Takayangagi Y, Nishiyama S, Takahasi T, Furuichi A, Kido M, et al. 2017; Increased frontal gyrification negatively correlates with executive function in patients with first-episode schizophrenia. *Cerebral Cortex*. 27(4):2686–2694. DOI: 10.1093/cercor/bhw101 [PubMed: 27095825]
33. Miller TJ, McGlashan TH, Rosen JL, Cadenhead K, Ventura J, McFarlane W, Woods SW. 2003; Prodromal assessment with the structured interview for prodromal syndromes and the scale of prodromal symptoms: Predictive validity, interrater reliability, and training to reliability. *Schizophrenia Bulletin*. 29(4)doi: 10.1093/oxfordjournals.schbul.a007040
34. Miller TJ, McGlashan TH, Woods SW, Stein K, Driesen N, Corcoran CM, et al. 1999; Symptom assessment in schizophrenic prodromal states. *Psychiatric Quarterly*. 70(4):273–287. [PubMed: 10587984]
35. Wilkinson GS, Robertson GJ. 2006 Wide range achievement test 4 (WRAT4). Psychological Assessment Resources.
36. Revelle, W. Package “psych”. 2017. Retrieved, 2017, from [http://personalityproject.org/r/psych\\_manual.pdf](http://personalityproject.org/r/psych_manual.pdf)
37. Bakker G, Caan MWA, Vingerhoets WAM, Da Silva-Alves F, De Koning M, Boot E, et al. 2016; Cortical morphology differences in subjects at increased vulnerability for developing a psychotic disorder: A comparison between subjects with ultra-high risk and 22q11.2 deletion syndrome. *PLoS ONE*. 11(11):1–16. DOI: 10.1371/journal.pone.0159928
38. Hirjak D, Kubera KM, Wolf RC, Thomann AK, Hell SK, Seidl U, Thomann PA. 2015; Local brain gyrification as a marker of neurological soft signs in schizophrenia. *Behavioural Brain Research*. 292:19–25. DOI: 10.1016/j.bbr.2015.05.048 [PubMed: 26031380]
39. Palaniyappan L, Marques TR, Taylor H, Mondelli V, Reinders AAT, Bonaccorso S, et al. 2016; Globally efficient brain organization and treatment response in psychosis: A connectomic study of gyrification. *Schizophrenia Bulletin*. 42(6):1446–1456. DOI: 10.1093/schbul/sbw069 [PubMed: 27352783]
40. White T, Andreasen NC, Nopoulos P, Magnotta V. 2003; Gyrification abnormalities in childhood- and adolescent-onset schizophrenia. *Biological Psychiatry*. 15(4):418–426. DOI: 10.1016/S0006-3223(03)00065-9
41. Cho KIK, Shenton ME, Kubicki M, Jung WH, Lee TY, Yun JY, et al. 2016; Altered thalamo-cortical white matter connectivity: Probabilistic tractography study in clinical-high risk for psychosis and first-episode psychosis. *Schizophrenia Bulletin*. 42(3):723–731. [PubMed: 26598740]
42. Csernansky JG, Gillespie SK, Dierker DL, Anticevic A, Wang L, et al. 2008; Symmetric abnormalities in sulcal patterning in schizophrenia. *NeuroImage*. 43(3):440–446. DOI: 10.1016/j.neuroimage.2008.07.034 [PubMed: 18707008]
43. Karlsgodt KH, Sun D, Cannon TD. 2010; Structural and functional brain abnormalities in schizophrenia. *Current Directions in Psychological Science*. 19(4):226–231. DOI: 10.1177/0963721410377601 [PubMed: 25414548]
44. Pruessner M, Cullen AE, Aas M, Walker EF. 2017; The neural diathesis-stress model of schizophrenia revisited: An update on recent findings considering illness stage and neurobiological and methodological complexities. *Neuroscience & Biobehavioral Reviews*. 73:191–218. [PubMed: 27993603]
45. Collin G, van den Heuvel MP. 2013; The ontogeny of the human connectome. *The Neuroscientist*. 19(6):616–628. DOI: 10.1177/1073858413503712 [PubMed: 24047610]
46. Mittal VA, Gupta T, Orr JM, Pelletier AL, Dean DJ, Lunsford-Avery JR, Millman ZB. 2013; Physical activity level and medial temporal health in youth at ultra high-risk for psychosis. *Journal of Abnormal Psychology*. 122(4):1101–1110. DOI: 10.1037/a0034085 [PubMed: 24364613]
47. Mendez M, Popkin B. 2004; Globalization, urbanization, and nutritional change in the developing world. *Globalization of food systems in Developing Countries: Impact on food security and nutrition*. 5580
48. Filatova S, Koivumaa-Honkanen H, Hirvonen N, Freeman A, Ivandic I, Hurtig T, et al. 2017; Early motor developmental milestones and schizophrenia: A systematic review and meta-analysis. *Schizophrenia Research*. 188:13–20. DOI: 10.1016/j.schres.2017.01.029 [PubMed: 28131598]

49. Bloemen OJN, de Koning MB, Schmitz N, Nieman DH, Becker HE, de Haan L, et al. 2010; White-matter markers for psychosis in a prospective ultra-high-risk cohort. *Psychological Medicine*. 40(8):1297–1304. DOI: 10.1017/S0033291709991711 [PubMed: 19895720]
50. Peters BD, Blaas J, de Haan L. 2010; Diffusion tensor imaging in the early phase of schizophrenia: What have we learned? *Journal of Psychiatric Research*. 44(15):993–1004. [PubMed: 20554292]
51. von Hohenberg CC, Pasternak O, Kubicki M, Ballinger T, Vu MA, Swisher T, Shenton ME. 2014; White matter microstructure in individuals at clinical high risk of psychosis: A whole-brain diffusion tensor imaging study. *Schizophrenia Bulletin*. 40(4):895–903. DOI: 10.1093/schbul/sbt079 [PubMed: 23737549]
52. Walterfang M, McGuire PK, Yung AR, Phillips LJ, Velakoulis D, Wood SJ, et al. 2008; White matter volume changes in people who develop psychosis. *The British Journal of Psychiatry: The Journal of Mental Science*. 193(3):210–215. DOI: 10.1192/bjp.bp.107.043463 [PubMed: 18757979]
53. Abramovic L, Boks MP, Vreeker A, Bouter DC, Kruiper C, Verkooijen S, et al. 2016; The association of antipsychotic medication and lithium with brain measures in patients with bipolar disorder. *Eur Neuropsychopharmacol*. 26(11):1741–1751. [PubMed: 27665062]
54. Jørgensen KN, Nesvåg R, Gunleiksrud S, Raballo A, Jönsson EG, Agartz I. First- and second-generation antipsychotic drug treatment and subcortical brain morphology in schizophrenia. *Eur Arch Psychiatry Clin Neurosci*. 266(5):451–460.
55. deWit S, Ziermans TB, Nieuwenhuis M, Schothorst PF, van Engeland H, Kahn RS, et al. 2017; Individual prediction of long-term outcome in adolescents at ultra-high risk for psychosis: Applying machine learning techniques to brain imaging data. *Human Brain Mapping*. 38(2):704–714. DOI: 10.1002/hbm.23410 [PubMed: 27699911]
56. Insel TR. 2010; Rethinking schizophrenia. *Nature*. 468(7321):187–193. DOI: 10.1038/nature09552 [PubMed: 21068826]
57. Mihailov A, Padula MC, Scariati E, Schaer M, Eliez S. 2017; Morphological brain changes associated with negative symptoms in patients with 22q11.2 Deletion Syndrome. *Schizophrenia Research*. 188:52–58. [PubMed: 28139357]
58. Pantelis C, Yücel M, Wood SJ, Velakoulis D, Sun D, Berger G, McGorry PD. 2005; Structural brain imaging evidence for multiple pathological processes at different stages of brain development in schizophrenia. *Schizophrenia Bulletin*. 31(3):672–696. DOI: 10.1093/schbul/sbi034 [PubMed: 16020551]



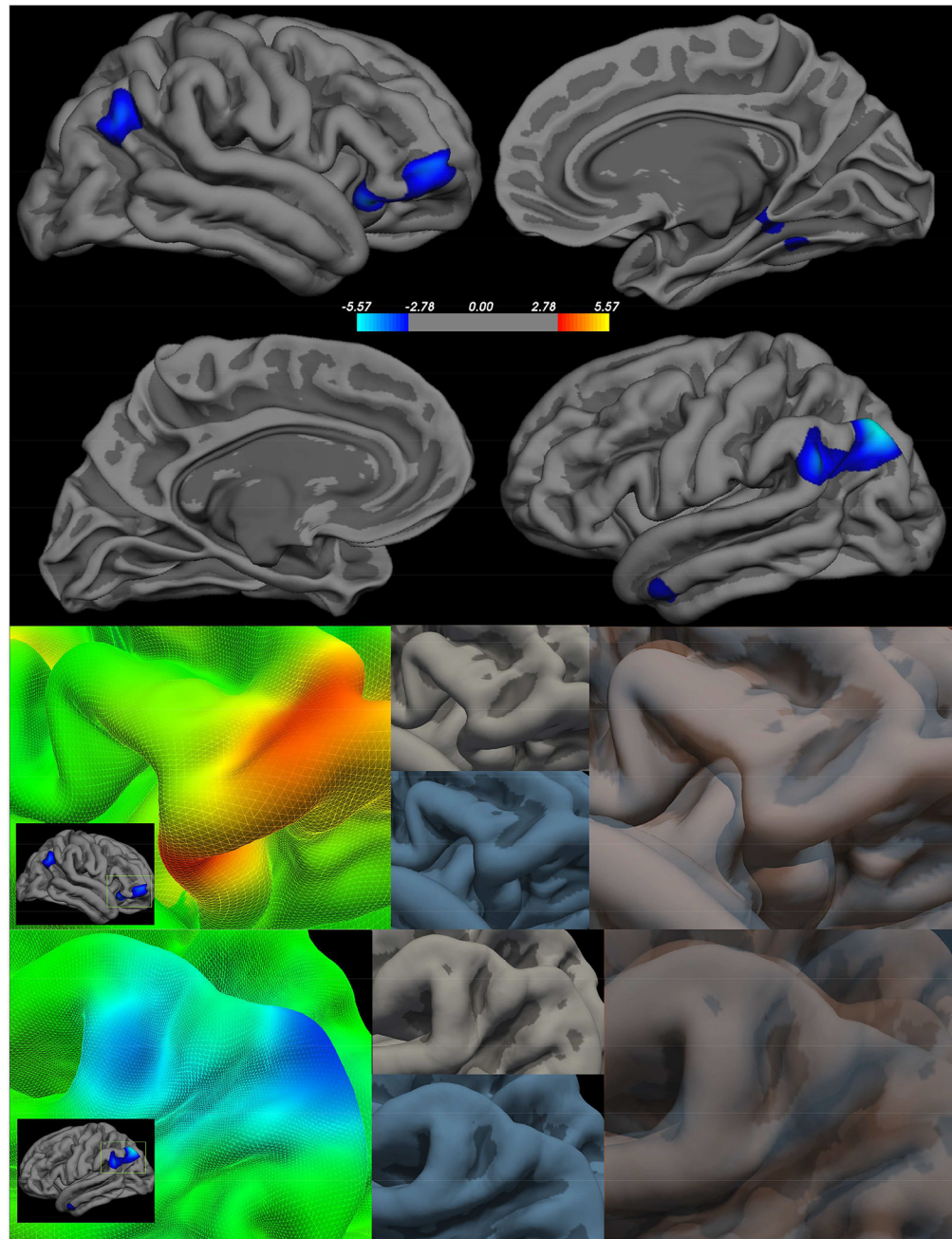


**Figure 1. Clinical High Risk > Healthy Controls - local Gyrfication Index**

Right Hemisphere (first panel top) Left Hemisphere FDR (first panel bottom) - FDR corrected  $p < 0.05$ ; Peak clusters are highlighted in the second panel (group statistical image left) to demonstrate how each feature varies between the CHR (group average in blue lower center) and HC (group average upper center in gray), which were then overlaid to highlight the surface differences.

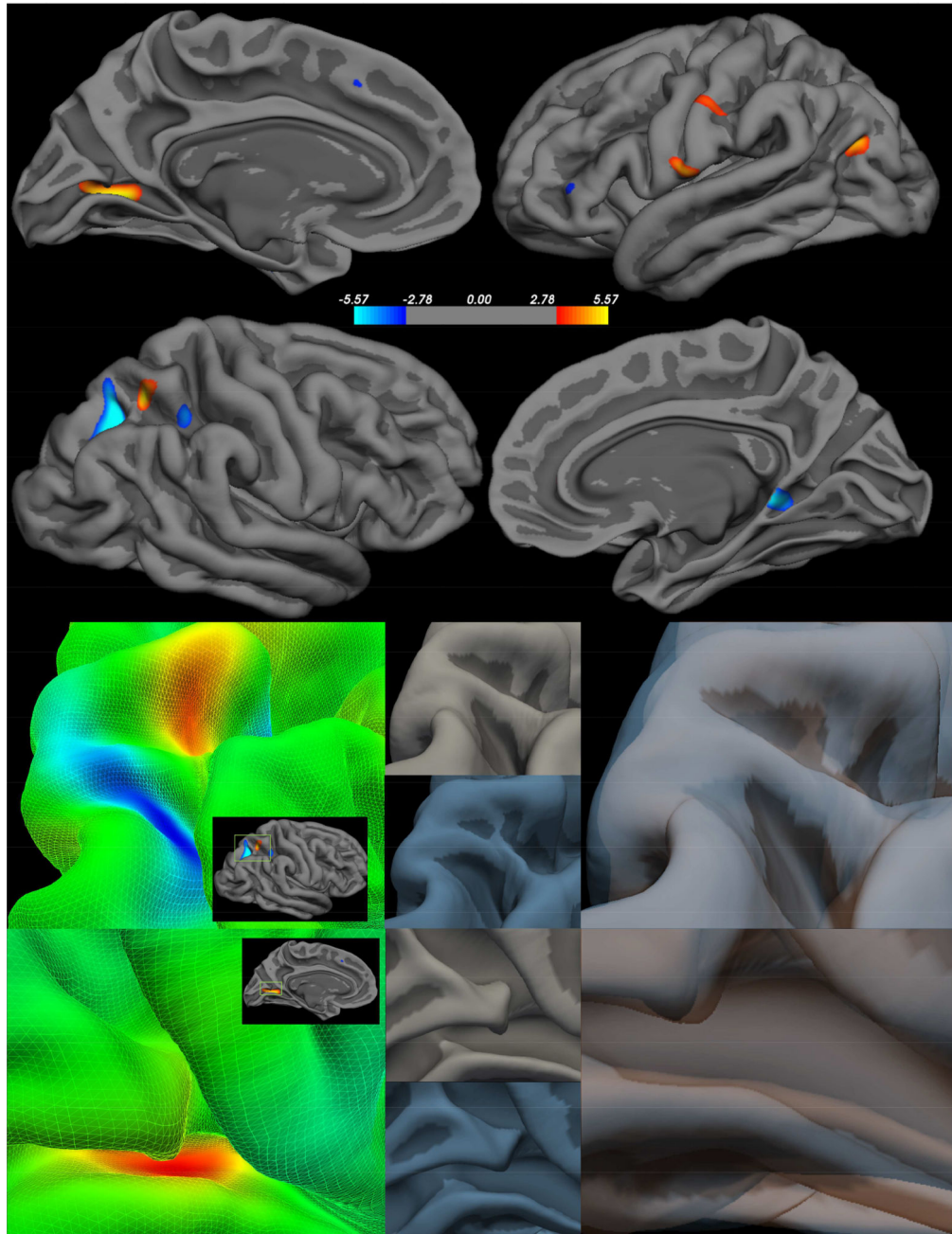


**Figure 2. Clinical High Risk > Healthy Controls – Mean Curvature Index (MCI)**  
 Right Hemisphere (first panel top) Left Hemisphere FDR (first panel bottom) - FDR corrected  $p < 0.05$ ; Peak clusters are highlighted in the second panel (group statistical image left) to demonstrate how each feature varies between the CHR (group average in blue lower center) and HC (group average upper center in gray), which were then overlaid to highlight the surface differences.



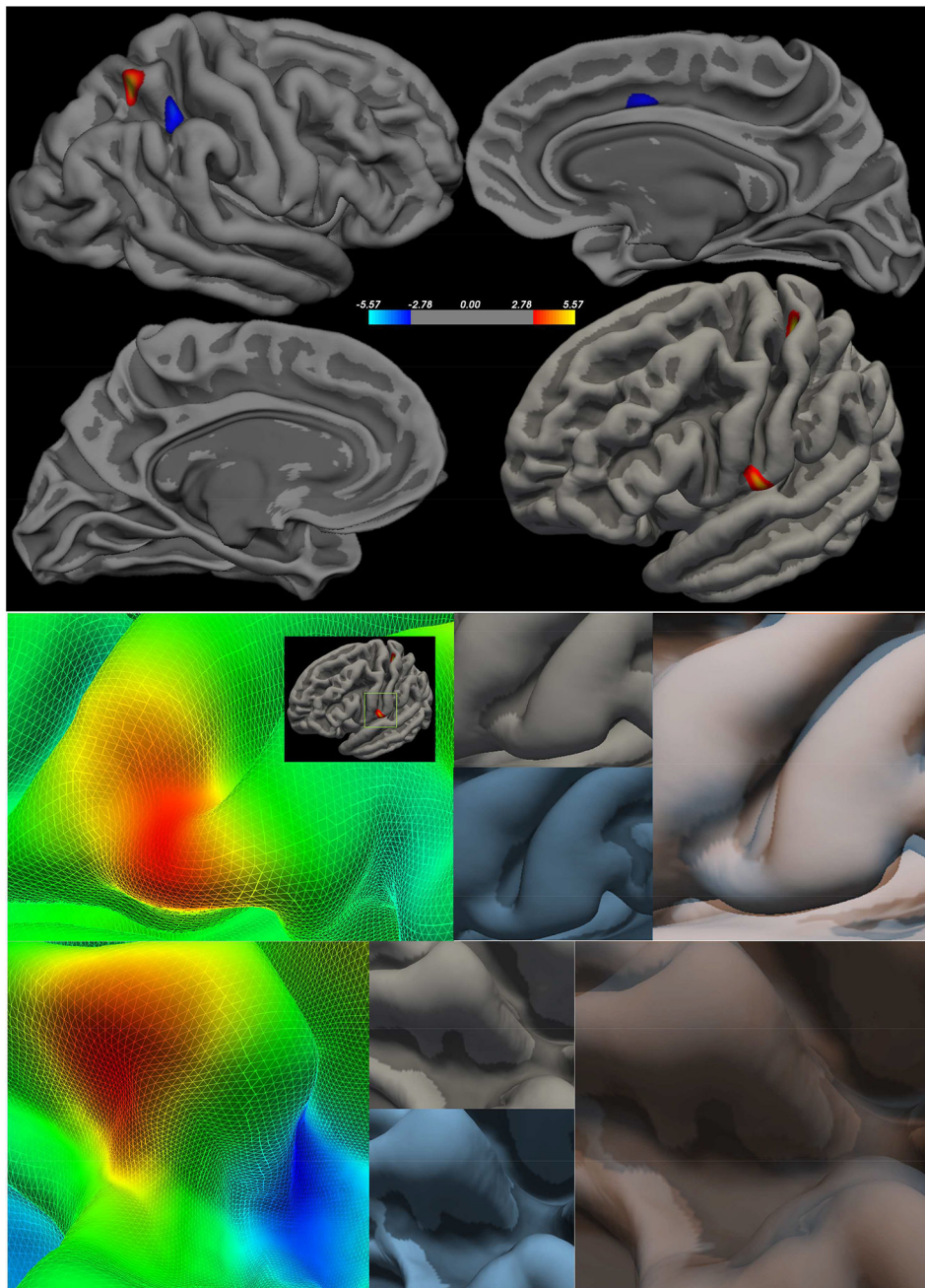


**Figure 3. Clinical High Risk > Healthy Controls – Sulcal Depth**

Right Hemisphere (first panel top) Left Hemisphere FDR (first panel bottom) - FDR corrected  $p < 0.05$ ; Peak clusters are highlighted in the second panel (group statistical image left) to demonstrate how each feature varies between the CHR (group average in blue lower center) and HC (group average upper center in gray), which were then overlaid to highlight the surface differences.

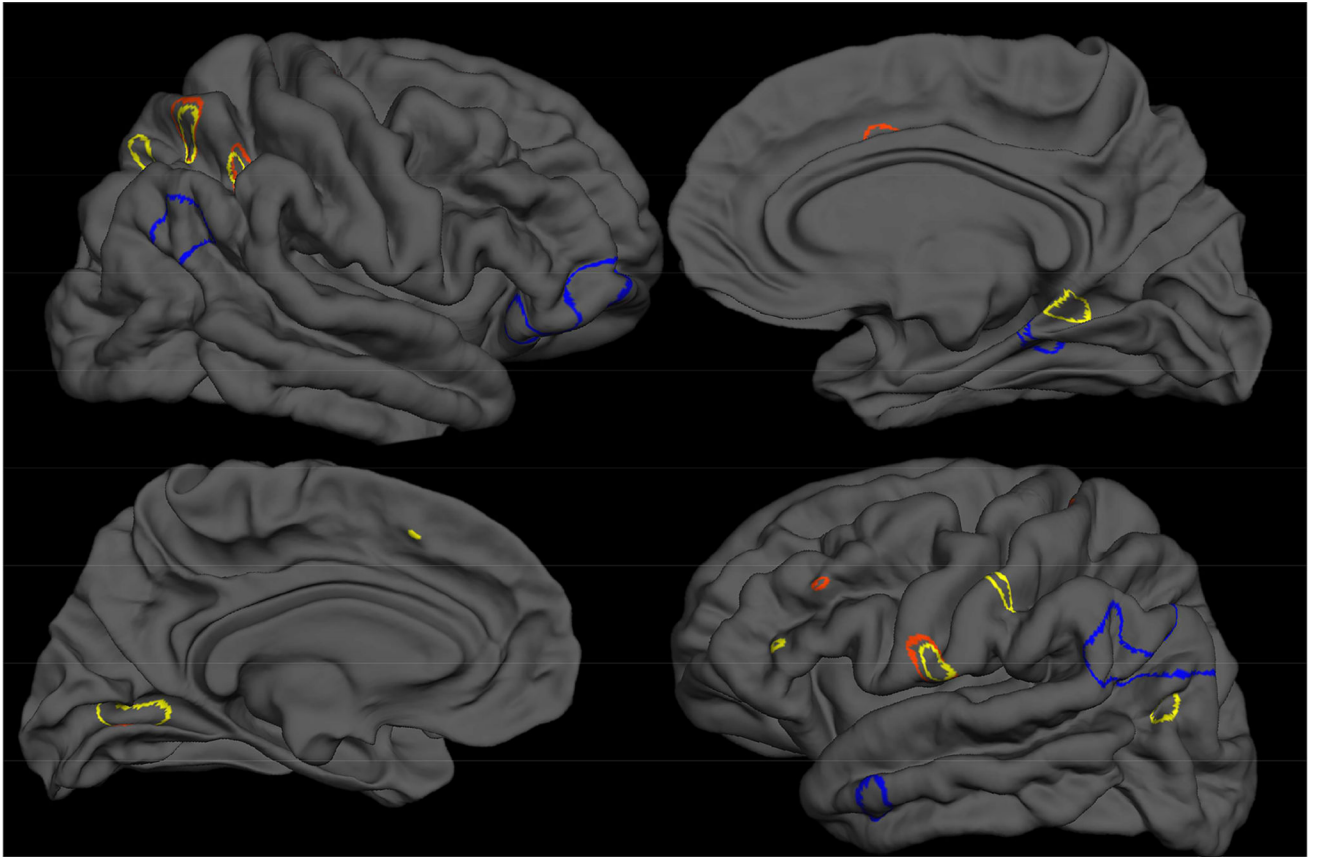


**Figure 4. Overlap of Significance Clusters**  
Local Gyration Index - LGI (blue), Mean Curvature Index -MCI (yellow), and Sulcal Depth (red)

**Table 1**

## Review of Psychosis Literature on Gyrfication CSM

Author	N	Population	Metric	Findings
Harris et al., 2004a (15)	128	GHR	Gyrification Index	Related to Conversion
Harris et al., 2007 (30)	34	FEP	Gyrification Index	Abnormal at First Episode of psychosis
Kulynych et al., 1997 (12)	9	SZ	Gyrification Index	Found frontal hypergyrfication
Sasabayashi et al., 2017 (31)	104	CHR	GI	Related to Conversion
Sasabayashi et al., 2017 (32)	62	FEP	GI	Abnormal at First Episode of psychosis
Bakker et al., 2016 (37)	36	CHR n=18 22q11-deletion n=18	GI	Related to the 22q11-deletion
Mihailov et al., 2017 (56)	71	22q11-deletion	GI	Related to the 22q11-deletion
deWit et al., 2017 (54)	24	CHR	GI	Related to clinical severity at follow-up
Palaniyappan et al., 2011 (14)	57	SZ	GI	Found frontal hypogyrfication
Takahashi et al., 2013 (22)	64	FEP	Sulcal Depth	Related to deficits in executive function
Csernansky et al., 2008 (42)	33	SZ	Sulcal Depth	Found asymmetric sulcal depth in temporal lobes

Author Manuscript

Author Manuscript

Author Manuscript

Author Manuscript

Demographic characteristics. Positive, negative, and disorganized symptoms reflect total sums from domains from the Structured Interview for Prodromal Syndromes (SIPS).

**Table 2**

	<b>UHR</b>	<b>Control</b>	<b>Total</b>	<b>Statistic</b>	<b>P</b>
<b>Age</b>					
Mean (SD)	18.98 (1.30)	19.13 (1.51)	19.05 (1.40)	t (74)=-.49	.63
<b>Gender</b>					
Male	28	13	40	$\chi^2(1)=7.71$	.005
Female	15	25	41		
Total	43	38	81		
<b>Education (years)</b>					
Mean (SD)	12.67 (1.44)	13.05 (1.83)	12.85 (1.64)	t (70)=-1.04	.30
<b>Parent Education (years)</b>					
Mean (SD)	15.66 (2.89)	15.71 (2.60)	15.68 (2.74)	t (79)=-.08	.94
<b>Symptoms Domains</b>					
Mean (SD)					
Positive Baseline	11.72 (3.50)	.66 (1.40)	6.53 (6.18)	t (1, 79)=18.23	.001
Positive Follow-Up	10.44 (5.95)	.32 (.66)	5.69 (6.68)	t (1, 79)=10.44	.001
<b>Wide Range Achievement Test</b>					
Mean (SD)	108.88 (12.02)	104.40 (11.82)	106.79 (12.09)	t (73) = 1.62	.11

Talairach coordinates of regions showing group differences- comparing control participants relative to CHR participants - in local gyrification index.

**Table 3**

Talairach Coordinates						
Hemisphere	p-value	Size (mm <sup>2</sup> )	X	Y	Z	Region
Left	>0.00001	3285.18	-34.9	-69.5	45.4	Bank of the Superior Temporal Sulcus
	>0.001	351.98	-51.8	-0.2	-28.2	Temporal Pole
Right	>0.0001	1833.49	42.3	26.5	-14.4	Lateral Orbitofrontal
	>0.0001	1163.56	49.5	-57.8	32.1	Bank of the Superior Temporal Sulcus
	>0.001	720.58	26.3	-42.1	-6.8	Parahippocampal Gyrus
	>0.001	30.13	47.9	-66.7	14.3	Fusiform

Talairach coordinates of regions showing group differences- comparing control participants relative to CHR participants - in mean curvature index (MCI).

**Table 4**

Talairach Coordinates						
Hemisphere	p-value	Size (mm2)	X	Y	Z	Region
Left	>0.00001	356.18	-21.8	-67.9	0.8	Lingual Gyrus
	>0.0001	148.75	-36.7	-13.2	-28.3	Fusiform
	>0.0001	136.46	-40.2	-71.3	20.5	Inferior Parietal
	>0.0001	69.97	-60.3	-7	11.8	Postcentral Gyrus
Right	>0.001	50.01	-57	-17.6	37.4	Postcentral Gyrus
	>0.000001	318.16	21.7	-65.5	37.5	Superior Parietal Lobule
	>0.0001	182.77	26.7	-54.2	53.8	Superior Parietal
	>0.0001	116.57	13.5	-42.3	-0.3	Isthmus Cingulate
	>0.0001	67.43	32.4	-44	44.5	Superior Parietal



Talairach coordinates of regions showing group differences- comparing control participants relative to CHR participants - in sulcal depth

**Table 5**

Talairach Coordinates						
Hemisphere	p-value	Size (mm2)	X	Y	Z	Region
Left	>0.00001	259.45	-35.3	-30.8	58.3	Postcentral Gyrus
	>0.00001	137.32	-59.9	-6.7	11.7	Postcentral Gyrus
	>0.00001	32.54	-10.7	-28.3	38.5	Posterior Cingulate
	>0.00001	20.1	-36.4	-13.4	-29.1	Fusiform Gyrus
	>0.00001	13.85	-44.2	32.4	23.2	Rostral Middle Frontal
Right	>0.00001	15.89	-7.2	-72.2	4	Lingual Gyrus
	>0.00001	238.92	28.4	-54.1	58.2	Superior Parietal
	>0.00001	212.01	31.7	-43.4	45.2	Superior Parietal
	>0.00001	94.53	11	13.5	34.5	Caudal Anterior Cingulate